Experimental investigation and numerical simulations of the cylindrical machining of a Ti-6Al-4V tree

M. Sahli[1], D. Bassir[2], B. Guo[3]; T. Barriere[4], G. Chen[3]

[1] Normandie Univ, ENSICAEN, UNICAEN, CEA, CNRS, CIMAP, 14000 Caen, France

[2] UBFC, UTBM, UMR–CNRS 5060, Rue de Leupe, 90010 Belfort Cedex, France

[3] Guangdong University of Technology, Faculty of Civil Engineering, Chine

[4] University Bourgogne-Franche-Comté, COMUE UBFC, Femto-ST Institute, Department of Applied Mechanics, 24 Rue de l'Epitaphe, 25030 Besançon, France

Abstract

Predicting the behaviour of the Ti-6Al-4V alloy during the turning operation was very important in the choice of suitable cutting tools and also in the machining strategies. In this stady, a 3D model with thermo-mechanical coupling has been proposed to study the influence of cutting parameters and also lubrication on the performance of cutting tools. The constants of the constitutive Johnson-Cook model of Ti-6Al-4V alloy were identified using inverse analysis based on the parameters of the orthogonal cutting process. Then, numerical simulations of the finishing machining operation were developed and experimentally validated for the cylindrical stock removal stage with the finishing cutting tool.

Keywords: Titanium turning, cutting tools, FE simulation, chip.

1. Introduction

Metal chip removal machining was frequently used in the mechanical fabrication industry [1-4]. It makes it possible to obtain parts of complex shape characterized by a low roughness of the surface states at a fairly low cost, etc. Some alloys such as super alloys based Cr, Ni and Ti are machined in a conventional manner and lead to rapid wear of the edges of cutting inserts for their high strength and abrasiveness, even at fairly high cutting speeds. Their low thermal conductivity therefore prevents the dissipation of the heat generated by the cutting, which causes a rapid increase in the heat increase of the workpiece [5-7]. This leads to early damage of the cutting insert and directly affects the final quality of the workpiece and its machined surface [8,9]. In this context, it was interesting to propose a reliable 3D FE model which allows us a better understanding of the cutting insert-part interaction during the machining of this type of alloys.

Numerical simulation of machining process and the residual stresses induced by the cutting operation have been investigated by many researchers [10-15]. Takahashi et al. (2015) studied numerically analyzed the influence of the rotational speed of the workpiece on the sense of chip flow and the cutting force of tools during turning process [3]. It was concluded that the machining force significantly reduced by increasing the rotational speed of the tool when the sense of chip flow was tilted towards the direction of the tool rotation. Zhao (2011) proposed a 2D model to study the orthogonal cutting of SiCp/2024Al [16]. It was observed that the interaction of the tool with the elements of the reinforcement is the main reason for the defects observed on the machining surface and the wear of the cutting inserts. The modeling of metal cutting has therefore proved to be particularly complex due to the diversity of the physical phenomena involved, in particular thermomechanical coupling, contact / friction and material rupture. This is because during filming, plastic deformation and friction work are the main sources of heat in the processing area and can significantly increase the temperature in the cutting area. This increase in temperature can significantly affect various mechanical and thermal properties of the material of the part.

In this study, machining tests of Ti-6Al-4V alloy under starved of full lubrication were performed at different cutting speeds using conventional tools. We also focused on the investigation of the effects of cutting on cutting performance in terms of cutting forces and coefficient of friction. Then, 3D model with thermo-mechanical coupling has been proposed to study the influence of cutting parameters on the performance of cutting tools. This model was allowed us on the one hand to study the chip formation and on the other hand, to predict the stresses distributions, cutting forces and temperatures evolutions in the workpiece and the cutting insert.

2. Materials and experimental methods

2.1. Materials

Machining experiments were carried out on a cylindrical part made of wrought titanium alloy (Ti-6Al-4V) with a diameter of 50 mm and a length of 200 mm. In these tests, cemented carbide cutting inserts supplied by Sandvik Company were used. These GC6050 type inserts with a titanium-aluminum nitride (TiAlN) coating have been tested under different cutting conditions. The physical characteristics of the material to be machined and those of the cutting inserts are shown in Tables 1 and 2.

Proprieties	**Workpiece (Ti6Al4V)**	**Tool (Wc-Co)**
Density [Kg/m^3]	4430	15700
Young's modulus [MPa]	1.13xe5	6.50xe5
Poisson ratio	0.34	0.25
Thermal conductivity [w/m°C]	K(T)	91
Specific heat capacity [J/kg°C]	C_p(T)	206

Table 1. Material characteristics for the cylindrical bar and the cutting insert used in FE simulations.

Proprieties/Temperature [°C]	0	250	500	750	1000	1250	1500
K(T) [w/m°C]	6.651	6.996	8.591	8.591	15.031	19.106	22.286
C_p(T) [J/kg°C]	483.3	535.8	588.3	640.8	600.19	645.2	690.2

Table 2. Temperature dependent properties of titanium alloy [17].

2.2. Experimental methods

The effects of cutting on machining performance were studied and carried-out on a CNC CTX 320 Linear Gildemeister lathe under diffirent cutting conditions and with starved or full lubrication. The cutting experiments were stopped after a cutting length of 100 mm and the chips were collected.

A dynamometer (Kistler Co., Ltd., 9257B) was used to measure the values of cutting force in the machining experiments. All the tests were carried out using the following parameters: feed rate f = 0.2 mm/revolution; cutting depth a_p = 0.5 mm; cutting speed 40-200 m/min.

3. Experimental results and discussion

Figure 1 illustrates the evolution of the cutting force for textured tools, during the machining phase under conditions lubricated by full or starved fluid. It can be observed that the experimental values of the recorded machining force are very stable during the machining phase under conditions of complete lubrication. The same values of the three cutting force components remained constant using starved lubrication in the interval between the first 30 to 40 s; then an increase was observed around 20% to 24% (see Fig.1).

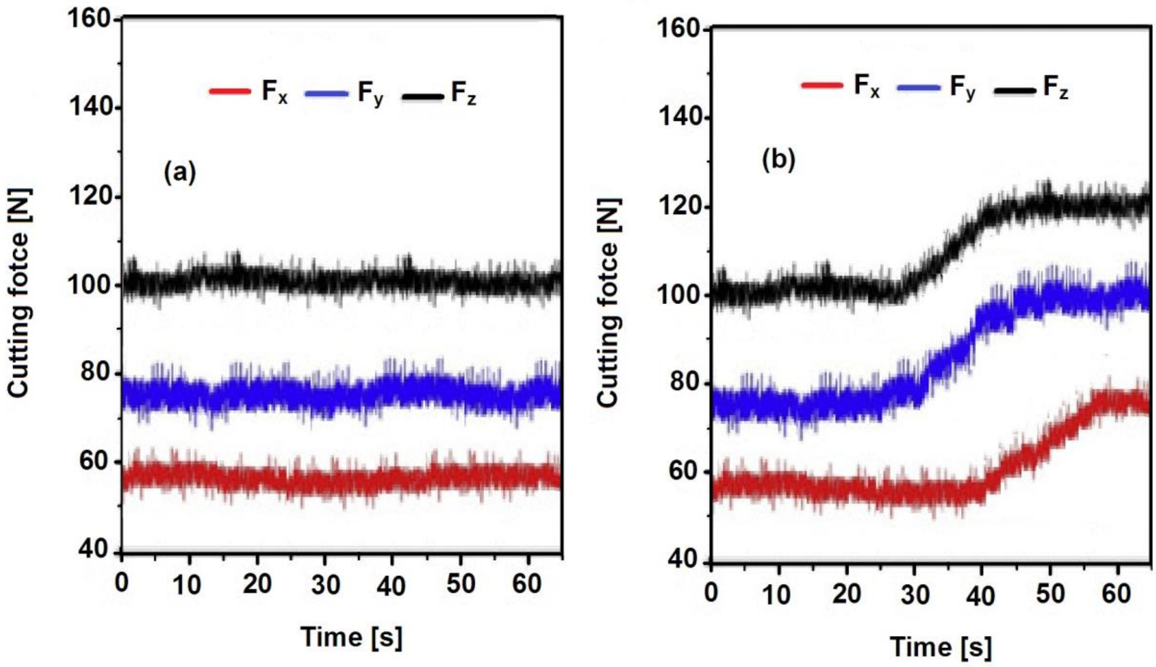

,

Fig.1. Cutting forces evolution vs. time in textured cutting surface under (a) full lubrication and (b) starved lubrication (cutting velocity: 160 m/min).

Figure 2 shows the evolution of the three components of the force values of the cutting tools measured at different cutting speeds varying from 40 to 200 m/min during the turning operation carried out under two different lubrication conditions either with full lubrication or without lubrication were considered. The cutting speed significantly affected the cutting force of the cutting inserts. The cutting behavior of the tools decreased in both cases of lubrication of the order of 7% to 10%. Figure 3 shows the evolution of the coefficient of friction as a function of the cutting speed for the two conditions of complete and severe lubrication. The results obtained showed that the values of the coefficient of friction decreased from 5% to 7% when the cutting speed increased for the machining phase either under complete lubrication or even under insufficient lubrication. It is clear that full lubrication of the cutting tool improves tribological performance a little better.

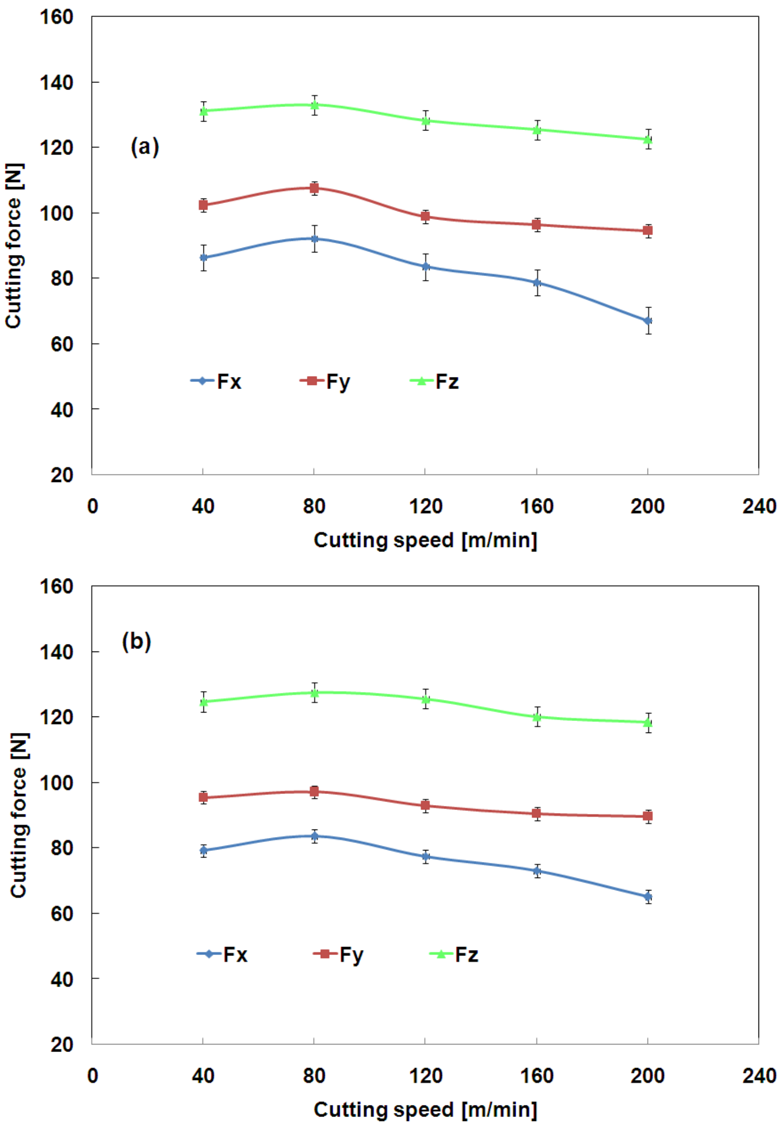

Fig.2. Evolution of cutting forces vs. cutting speeds obtained using textured cutting inserts under (a) complete fluid lubrication and (b) starved fluid lubrication.

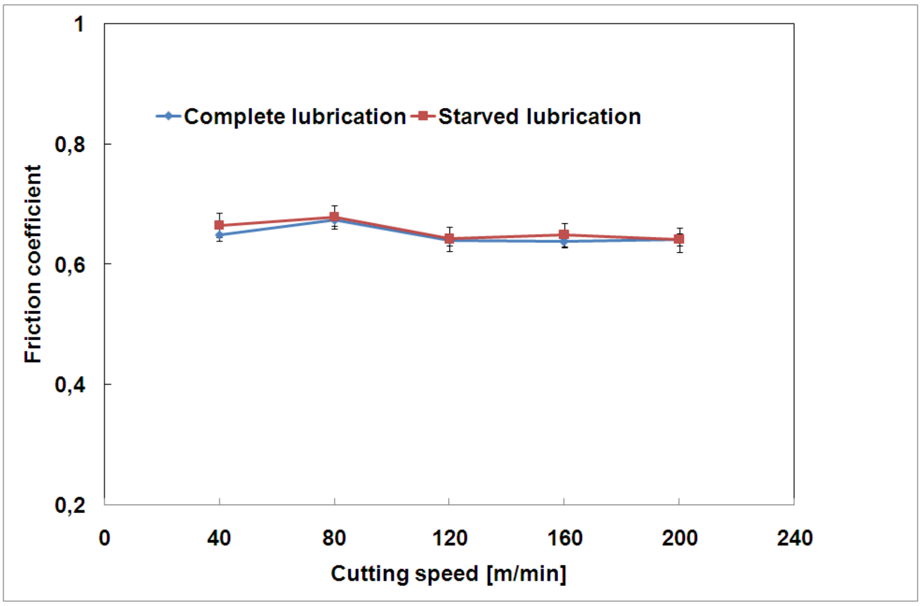

Fig.3. Friction coefficient vs. cutting speed of workpiece during machining process.

4. FE simulation of the turning process

4.1. Material constitutive model

The constitutive model of Johnson-Cook (JC) was utilised to modelling the mechanical behaviour of the material to be machined [18]. It allows thermo-mechanical coupling to be taken into account in this process in order to correctly allowing reproducing the thermo-mechanical phenomena interconnection in the cutting area.

$$\sigma = (A + B\varepsilon^n)\left[1 + Cln\left(\frac{\dot{\varepsilon}}{\dot{\varepsilon}_0}\right)\right]\left[1 - \left(\frac{T - T_0}{T_m - T_0}\right)^m\right]$$

where σ was the flow stress, ε was the true strain, $\dot{\varepsilon}_0$ was the reference true strain rate, $\dot{\varepsilon}$ was the true strain rate, T_0 was the ambient temperature, T_m was the workpiece material melting temperature, T was the workpiece temperature and (A, B, C, n, m) were the model constants.

Table 3 summarizes the Johnson-Cook parameters of Ti6Al4V alloy based on α phase using in our numerical analysis.

Yield strength A [MPa]	Hardening modulus B [MPa]	Hardening coefficient n	Strain rate sensitivity C	Thermal softening coefficient m	T_{melt} [°C]	T_{room} [°C]
889.37	683.71	0.451	0.035	1	1647	21

Table 3. Johnson-Cook material constants of titanium alloy used for FE simulations.

4.2. FE Turning process simulation

The 3D model developed in this work simulates the orthogonal cutting of an ordinary carbon steel cylindrical part made using a coated tungsten carbide cutting insert (K10). The geometric dimensions of the cylindrical bars considered in our 3D model were 200 mm in length by 50 mm in diameter. The geometry of the cutting insert was taken in accordance with a CNMA 120408 type cutting insert. The relative movement between the cylindrical bar and the cutting insert was simulated by a horizontal translational movement at constant speed. It is affected on all the nodes of the cutting tool, which is assumed to be rigid and undeformable. The nodes along the left and bottom sides of the cylindrical bars are fixed. In this study, different cutting speeds varying between 40 m/min and 200 m/min were tested. The cutting edge engagement length is 0.4mm.

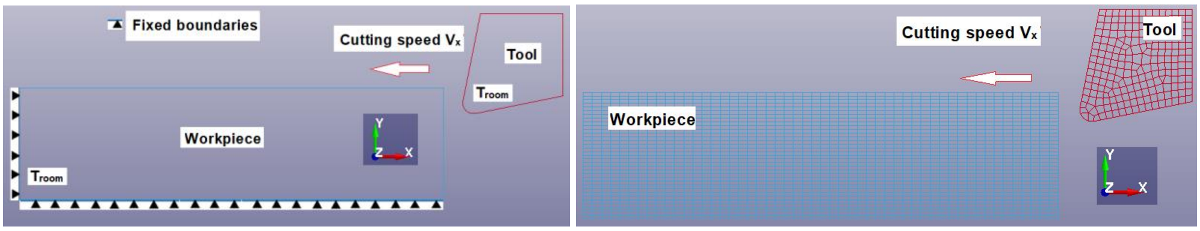

Fig.4. (a) CAD model of cutting insert and workpiece and (b) thermo-mechanical initial conditions of the cutting insert and workpiece for orthogonal cutting process.

The mechanical behavior of the cutting inserts is considered to be thermo-elastic while the titanium alloy has been taken into account thanks to the constitutive model J-C. The cylindrical bars and the cutting tool have been described with an adaptive mesh by 28,000 and 36,000 tetrahedron-mesh elements, respectively. Coulomb friction was used to model the friction with a coefficient value defined at the cylindrical bar-cutting insert interface in agreement with Bäker et al. (2002) and Calamaz et al. (2008). Figure 4 illustrates a descriptive diagram of the CAD of the initial geometry and the initial conditions and limits imposed.

5. Numerical simulations and discussion

The Von Mises stress isovalues at a time step of 3 s are illustrated in figure 5. The stresses are more and more distributed in the cut zone. It is clearly seen that the stress concentration zone is located near the cutting edge. The results also indicate that chips along the shear plane experience greater stresses. It was also important to numerically study the chip formation clockwork to see if the developed EF model was able to reproduce them according to the literature. Figure 6 shows the division of the shear band during the turning process, phenomenon related in the literature by Bäker et al. (2002). It has been observed that the shear was very localized in the form of a very narrow shear band which forms in two joining parts. This is because this shear band starts near the radius of the cutting edge of the tool and gradually spreads to the free surface of the workpiece. Then, it progresses from the free surface to the radius of the tool.

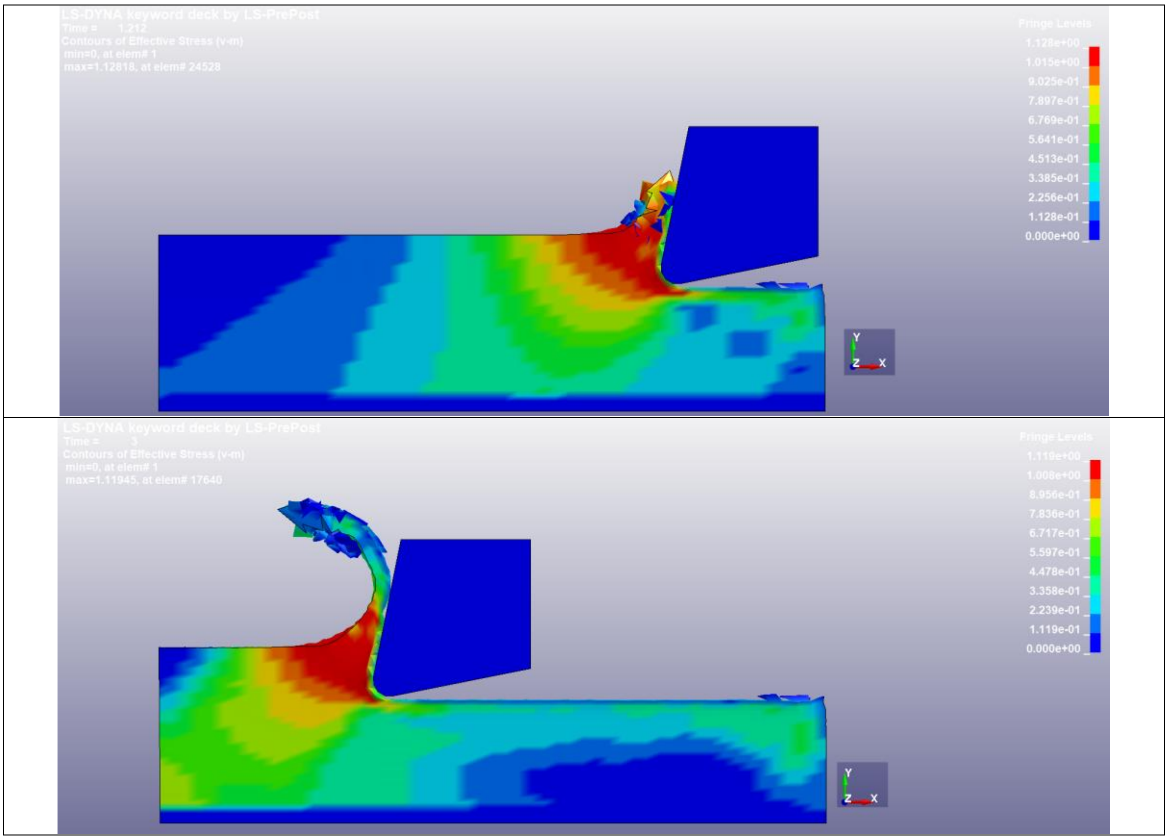

Fig.5. Von Mises stress distribution during chips formation

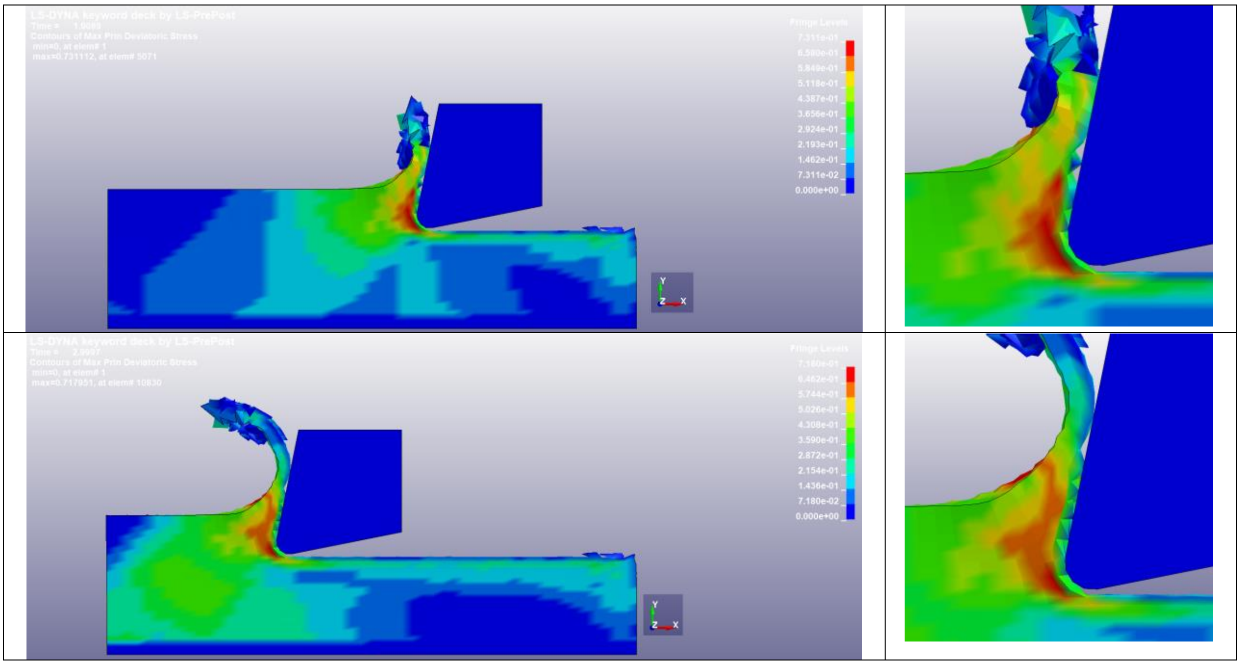

Fig.6. Shear band during chips formation.

Three cutting speed of 120 m/min, 160 m/min and 180 m/min were tested to study its influence on the final morphology of the chip (see Fig.7). The chip was found to be divided into two parts, one continuous and the other segmented. However, the more the cutting speed increases, the more the chip segmentation phenomenon becomes more and more pronounced. This is due, among other things, to the effect of thermal conduction located in the shear bands. This high heating greatly influences the stiffness of the material and therefore produces a more segmented chip. Figure 8 shows the temperature field at the interface, the shear zone and the cutting face of the tool when turning a Ti-6Al-4V cylindrical bar for different cutting speeds from 120 m/min to 200 m/min. It is clearly observed that the zone at maximum temperature was mainly detected at the level of the chip-cutter wafer contact zone and near the primary shear zone. The minimum cutting temperature obtained by the EF model was approximately 680 °C at 120 m/min and it increases significantly to a maximum of 533 °C at 200 m/min, recorded at the tool interface-chip (see Fig.8). In addition, several studies have indicated that often high temperatures can occur during the machining operation of this type of alloy classified as difficult to machine metal [1,19]. The low thermal conductivity of this alloy may explain this phenomenon caused by the trapping of heat produced locally in the cutting zone, resulting in a higher turning temperature [2,5].

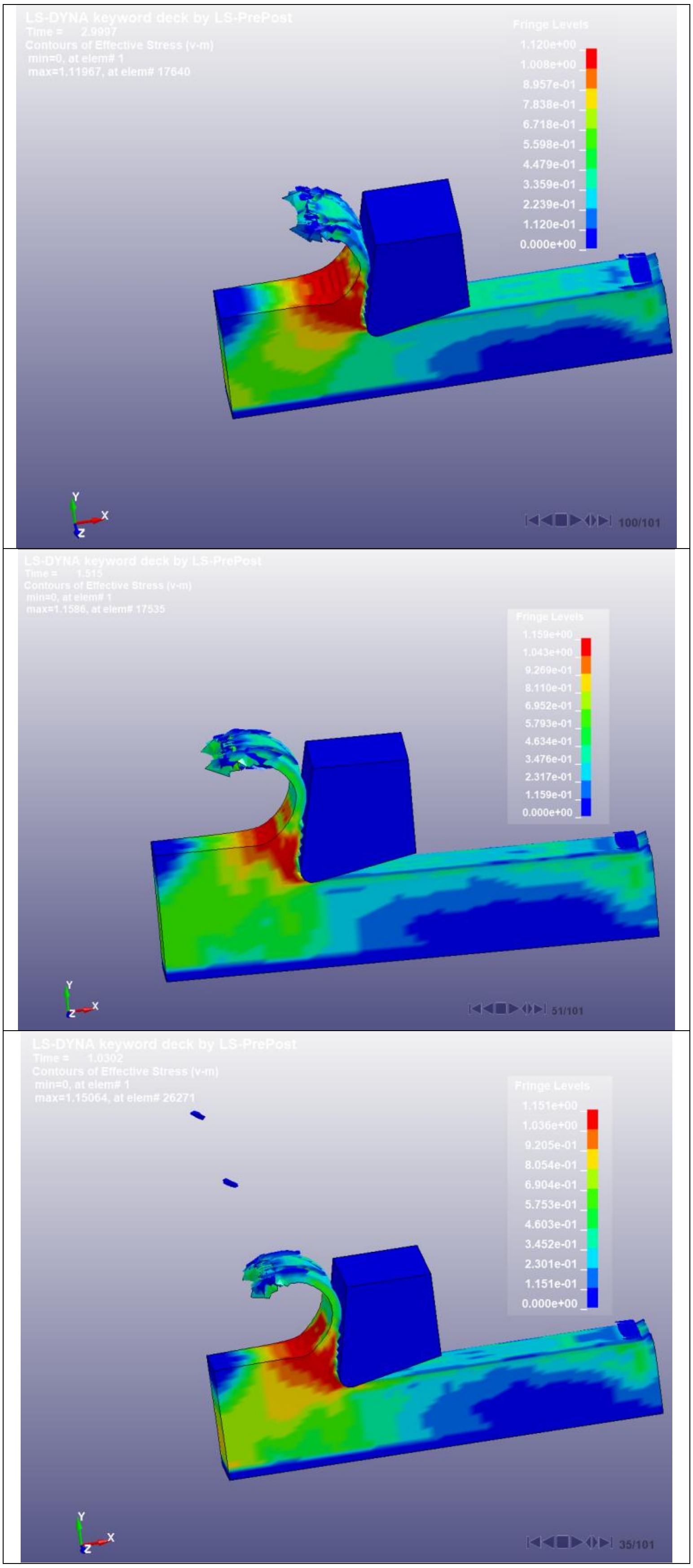

Fig.7. Effective stress distribution in chip according to cutting speed variation for starved lubrication ($\mu = 0.6$) and f = 0.2 mm/rev: (a) V_c = 120 m/min, (b) V_c = 160 m/min and (c) V_c = 180 m/min.

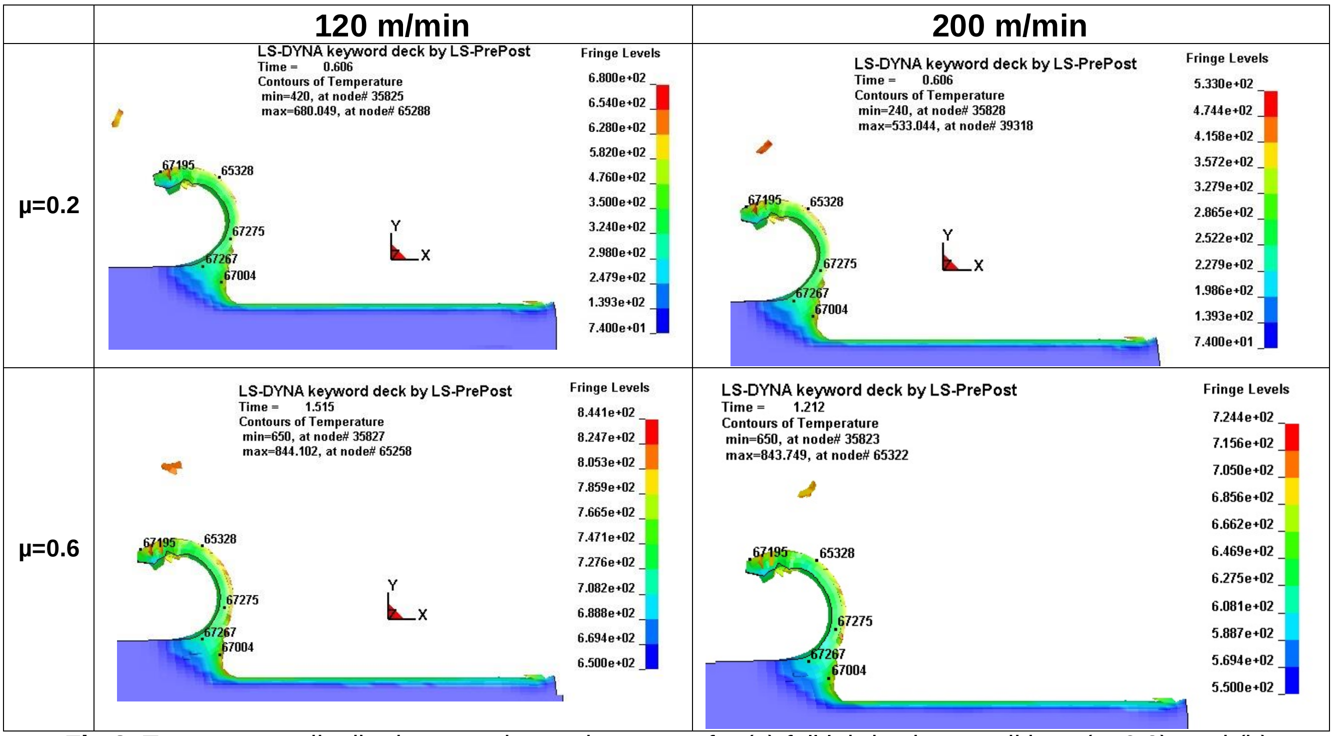

Fig.8. Temperature distribution over the cutting zones for (a) full lubrication conditions (μ=0.2), and (b) starved lubrication (μ=0.6).

To study the effect of the use of lubrication on the stress state of the Ti-6Al-4V part and the shape of the chips, friction values were taken into account, equal to 0.2 for a lubrication complete and 0.6 for severe machining at the insert cylindrical bar cutter interfaces. Figure 9 shows that there is a remarkable difference between the shape of the chips obtained when machining with full or severe lubrication. In machining condition with complete lubrication i.e. contact with very low friction, the final chip shape characterized by a radius of curvature at the interface of the cylindrical bar cutter insert was approximately 2, 5 lower than machining with severe lubrication. In addition, the thickness of the chips obtained by simulation in full lubrication was greater than that of machining with severe lubrication.

Moreover, it is interesting to indicate the weak influence of the coefficient of friction on the cutting force, as it is quite clear in Fig.10. This observation is predictable because the general shape of the chip remains almost the same whatever it is. lubrication conditions, that is, the value of the coefficient of friction. Indeed, during machining, energy will be transformed in the form of heat, which causes softening at the chip/tool interface, that is to say of the contact surfaces during turning. Similar trends were also indicated by Filice et al. (2006) and Calamaz et al. (2008).

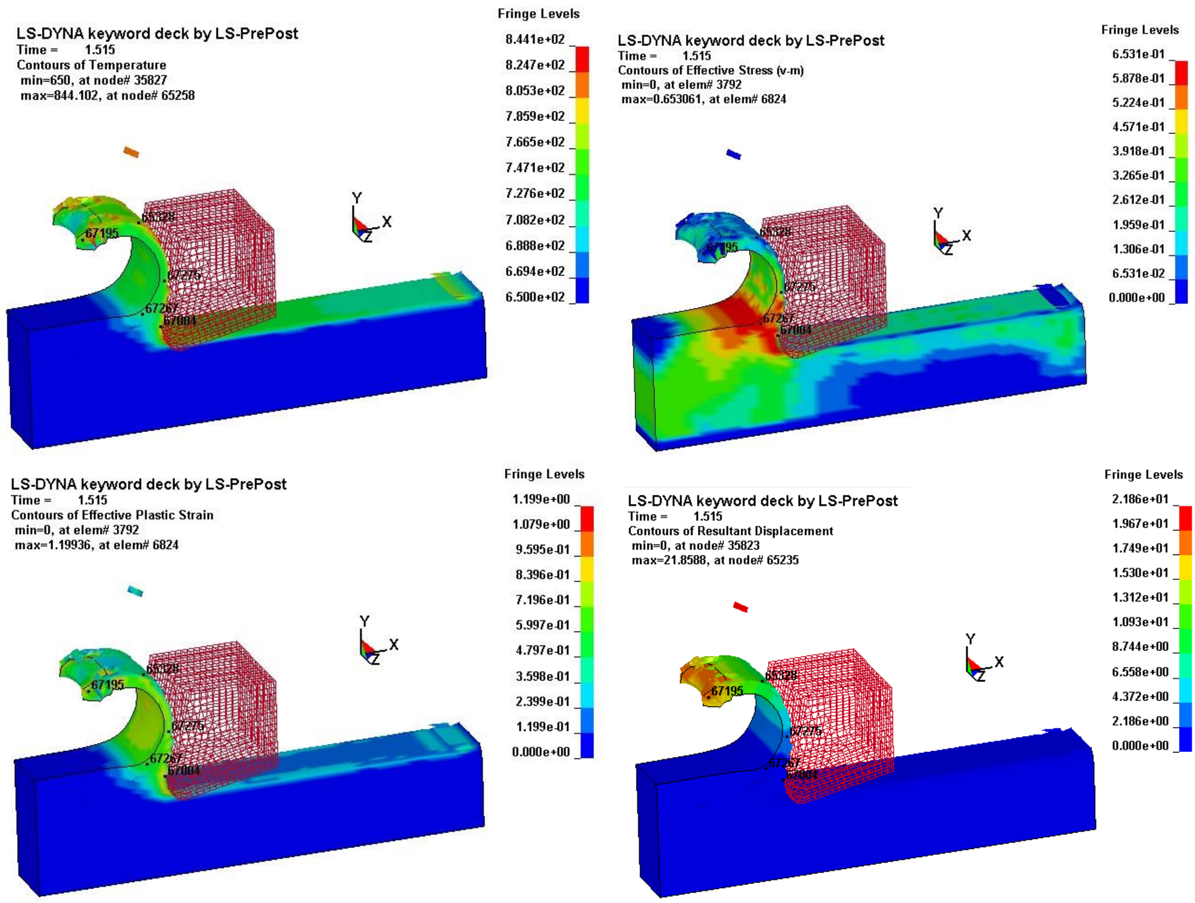

Fig.9. Numerical machining results in the cutting regions under starved lubrication conditions: (a) Temperature distributions, (b) Von-Mises stress, (c) Effective strain and (d) Resultant displacement (μ = 0.6, t =1.515 s, V_c = 200 m/min).

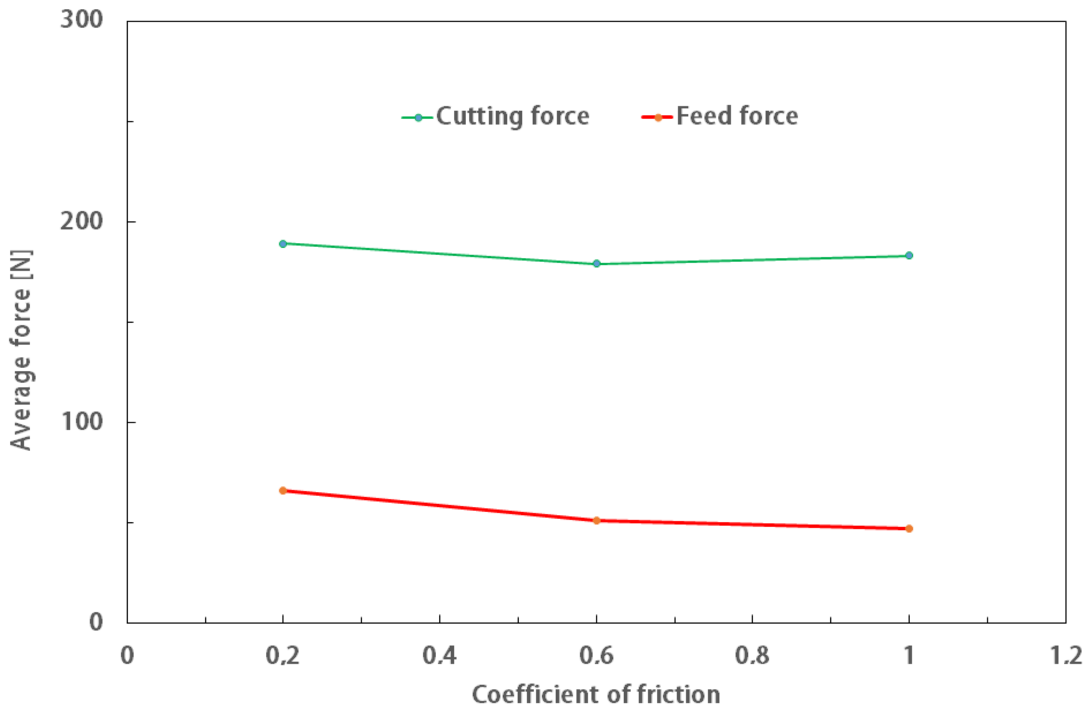

Fig.10. Evolution of the average cutting and feed forces versus coefficient of friction for f = 0.2 mm/rev, and V_c = 180 m/min.

6. Experimental validation

Figure 11 illustrates a comparative analysis of our numerical simulations and those resulting from the experimental results during the operation of turning the titanium alloy in conditions of full or starved lubricant. The same tendency is observed for the feed forces and the thrust forces generated during cutting. They are less noticeably affected by cutting speed. This variation is estimated between 175 ± 5N whatever the lubrication conditions. Also the friction coefficients also follow the same trend as those of the cutting forces whether for the experimental conditions as for those obtained in simulations (see Fig.12). In addition, we can see that our numerical data is slightly lower than the experimental data probably due to the complexity of the cutting conditions, the turning environment, and also due to the measurement error and vibrations not taken into account in our model. It can be concluded that the results provided by the 3D model are in good agreement under the two conditions of complete or starved lubrication with the experimental data with an error difference of only 5 to 10%.

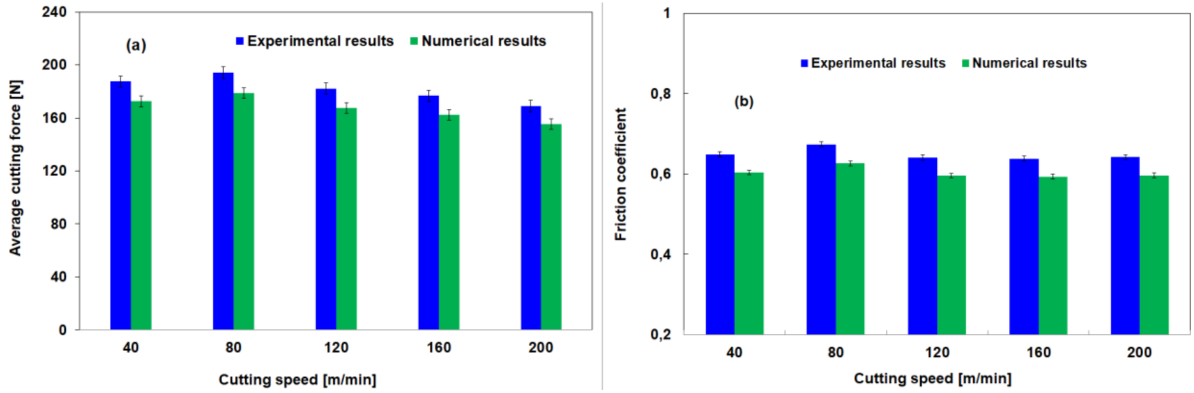

Fig.11. Comparison of experimental and simulated cutting forces under starved lubrication.

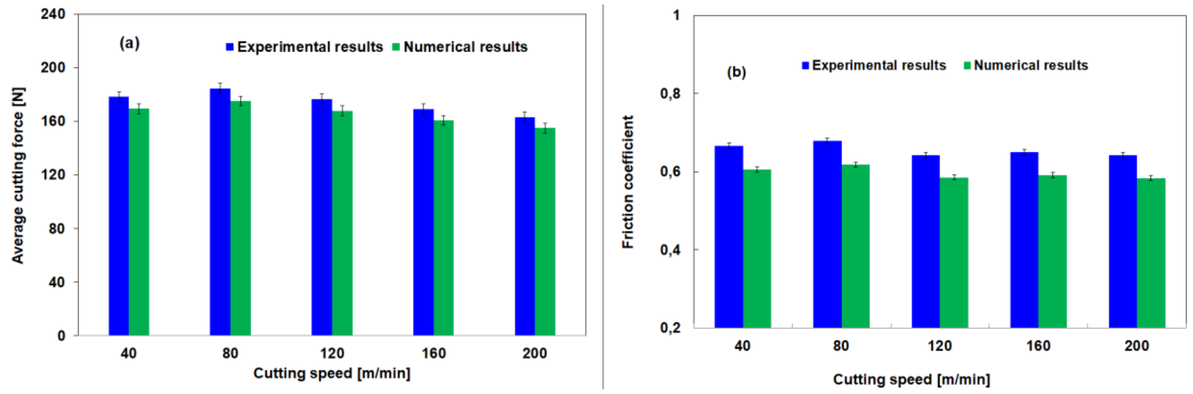

Fig.12. Comparison of experimental and simulated cutting forces under full lubrication conditions.

To complete our comparative analysis of the chip obtained and its morphology, measurements of the geometric characteristics of the shape of the chip were carried out and then studied. Three morphological data were used, namely the spacing of peaks, valleys and segments. It is noted that a well agreement was observed with mean relative errors close to 10% between our numerical data and the experimental results (see Table 4).

Cutting parameters		Chip morphology [µm]					
		Peak	Valley	Spacing	Peak	Valley	Spacing
		Full lubrication			Starved lubrication		
V=80 m/min	Experiments	200	110	75	210	115	84
	Simulations	181	105	69	173	107	71
	Relative error	9.5%	4.5%	8%	17.6%	6.9%	15.5%
V=120m/min	Experiments	193	103	69	198	109	73
	Simulations	176	98	63	179	101	65
	Relative error	8.8%	4.9%	8.7%	9.6%	4.9%	7.3%
V=160 m/min	Experiments	189	101	67	193	105	70
	Simulations	172	94	62	175	97	65
	Relative error	9%	6.9%	6%	9.3%	7.6%	7.1%

Table 4. Comparative results concerning chip morphology characteristics.

Based on comparison and analysis of the chip morphology and cutting force on the simulation and experiment, the two dimensional orthogonal cutting simulation model for Ti-6Al-4V alloy is reasonable and reliable. Thus, this model can be used to simulate and predict the actual machining process of Ti-6Al-4V alloy.

7. Conclusion

The numerical simulations proposed in this study allowed us to successfully predict the cutting forces under different lubrication conditions with some insignificant deviations at higher cutting speeds. The following conclusions can be expressed:

- The level of equivalent plastic deformations is 5 to 7% higher for high cutting speeds leading to more wavy chips;
- Turning is accompanied by considerable heat generation in the cutting zone, affecting material properties of the treated workpiece.
- The temperature in the cutting region is about 119° under starved lubrication lower due to the elimination of friction heating;
- The drop in process temperature was recorded for numerical simulations of cutting with reduced feed; this result is in good agreement with our experimental measurements and is explained by a reduced rate of material removal.

The results revealed that the model could correctly predict the cylindrical turning step with acceptable errors. The results of the numerical simulations show good agreement in the experimentally measured values of the machining experiments.

References

1. J. Barry, G. Byrne, D. Lennon, Observations on chip formation and acoustic emission in machining Ti–6Al–4V alloy. Int J Mach Tools Manuf, 41 (2001), pp. 1055-107.
2. M. Calamaz, D. Coupard, F. Girot, A new material model for 2D numerical simulation of serrated chip formation when machining titanium alloy Ti-6Al-4V. Int J Mach Tools Manuf, 48 (2008), pp. 275-288.

3. W. Takahashi, H. Sasahara, H. Yamamoto, Y. Takagi, FEM simulation on the effect of cutting parameters in the driven rotary cutting. Key Engineering Materials. Trans Tech Publications, 625 (2015), pp. 564-569.
4. M. Lotfi, H. Ashrafi, S. Amini, Farid, M. Jahanbakhsh, Characterization of various coatings on wear suppression in turning of Inconel 625: A three-dimensional numerical simulation. Proc. Inst. Mech. Eng. Part J: J. Eng. Tribol. (2016) 1350650116677131.
5. M. Nasr, E.-G. Ng, M. Elbestawi, Effects of workpiece thermal properties on machining-induced residual stresses-thermal softening and conductivity. Proc Inst Mech Eng B: J Eng Manuf, 221 (2007), pp. 1387-1400.
6. M. Bäker, J. Rosler, C. Siemers, A finite element model of high speed metal cutting with adiabatic shearing. Comput Struct, 80 (2002), pp. 495-513.
7. J. Liu, Y. K. Chou, Cutting tool temperature analysis in heat-pipe assisted composite machining. Journal of Manufacturing Science and Engineering: Transactions of the ASME 129 (2007) 902-910.
8. T. Wang, L. Xie, X. Wang, Simulation study on defect formation mechanism of the machined surface in milling of high volume fraction SiCp/Al composite. Int J Adv Manuf Technol, 79 (5-8) (2015), pp. 1185-1194.
9. J.W. Liu, K. Cheng, H. Ding, et al., Simulation study of the influence of cutting speed and tool-particle interaction location on surface formation mechanism in micromachining SiCp/Al composites. Proc Inst Mech Eng C J Mech Eng Sci, 232 (11) (2018), pp. 2044-2056.
10. U. Umer, M. Ashfaq, J. Qudeiri, et al., Modeling machining of particle-reinforced aluminum-based metal matrix composites using cohesive zone elements. Int J Adv Manuf Technol, 78 (5-8) (2015), pp. 1171-1179.
11. D.N. Zhang, Q.Q. Shangguan, C.J. Xie, et al., A modified Johnson-Cook model of dynamic tensile behaviors for 7075-T6 aluminum alloy. J Alloys Compd, 619 (2015), pp. 186-194.
12. Y.H. Zhao, Simulation and experimental study on the cutting process of SiCp/Al composites, Harbin Institute of Technology, Harbin (2011).
13. A. Li, J. Pang, J. Zhao, J. Zang, F. Wang, FEM-simulation of machining induced surface plastic deformation and microstructural texture evolution of Ti-6Al-4V alloy. International Journal of Mechanical Sciences, Vol. 123 (2017), pp. 214-223.
14. D.M. Kim, V. Bajpai, B.H. Kim, H.W. Park, Finite element modeling of hard turning process via a micro-textured tool. Int. J. Adv. Manuf. Technol. (2015), 10.1007/s00170-014-6747-x.
15. Y. Burhanuddin, S. Harun, G.A. Ibrahim, FEM simulation of machining AISI 1045 steel using driven rotary tool Appl. Mech. Mater. (2015), pp. 758.
16. L. Zhou, S. Huang, D. Wang, et al., Finite element and experimental studies of the cutting process of SiCp/Al composites with PCD tools. Int J Adv Manuf Technol, 52 (5-8) (2011), pp. 619-626.
17. Z. Chen, J. Zhang, P. Feng, Z. WuA simulation study on the effect of micro-textured tools during orthogonal cutting of titanium alloy Ti–6Al–4V, Appl Mech Mater, 281 (2013), pp. 389-394.
18. Johnson G, Cook W. A constitutive model and data for metals subjected to large strains, high strain rates and high temperatures. In: Proceedings of the seventh international symposium on ballistics. The Hague, The Netherlands; (1983) pp. 541-547.

19. D. Jianxin, W. Ze, L. Yunsong, Q. Ting, C. JiePerformance of carbide tools with textured rake-face filled with solid lubricants in dry cutting processes, Int. J. Refract. Met. Hard Mater., 30 (1) (2012), pp. 164-172.
20. L. Filice, D. Umbrello, S. Beccari, F. Micari, On the FE codes capability for tool temperature calculation in machining processes. Journal of Materials Processing Technology 174 (1-3) (2006) 286-292.